



Cite this: *J. Mater. Chem. C*, 2016, **4**, 8879

Received 12th August 2016,
Accepted 1st September 2016

DOI: 10.1039/c6tc03476d

www.rsc.org/MaterialsC

Naphtho[2,3-*b*]thiophene diimide (NTI): a mono-functionalisable core-extended naphthalene diimide for electron-deficient architectures†

Wangqiao Chen,^{abc} Masahiro Nakano,^{*a} Ji-Hoon Kim,^a Kazuo Takimiya^{*a} and Qichun Zhang^b

A new π -extended naphthalene diimide with one fused-thiophene ring, naphtho[2,3-*b*]thiophene diimide (NTI), was synthesized. Taking advantage of its mono-functionalisability, NTI was incorporated into various "NTI-terminated" π -conjugated architectures, which functioned as n-type organic semiconductors for field-effect transistors and solar cells.

Naphthalene diimide (NDI, Fig. 1), one of the imide-based π -extended structures, has been widely utilized in chromophores, supramolecular architectures, and electronic materials.¹ One of the effective ways to control the opto/electronic properties of NDI is to extend the π -system with fused aromatic or hetero-aromatic ring(s), which affords core-extended NDIs, often referred as cNDIs.² Whereas most of such cNDIs have two fused-(hetero)-aromatic rings on the naphthalene moiety, only a limited number of mono-(hetero)aromatic fused cNDIs have been reported,^{2b,c,f,j,k} and their utility as building blocks for opto/electronic materials has not been well explored. This is due to the difficulty of selective mono-functionalisation on the NDI core,³ which is in sharp contrast to perylene diimide (PDI) that has been extensively incorporated into various molecular architectures.⁴ For the elaboration of cNDI-based materials, it is desirable to develop mono-functionalisable cNDI-based building blocks. To this end, we have focused on mono-thiophene-fused NDI, namely naphtho[2,3-*b*]thiophene diimide (NTI, Fig. 1), since the thiophene α -position is a versatile handle for structural modifications. In fact, we have recently reported a cNDI with two fused-thiophene rings, *i.e.*, naphtho[2,3-*b*:6,7-*b'*]dithiophene diimide (NDTI, Fig. 1), which has been proved useful in developing NDTI-based

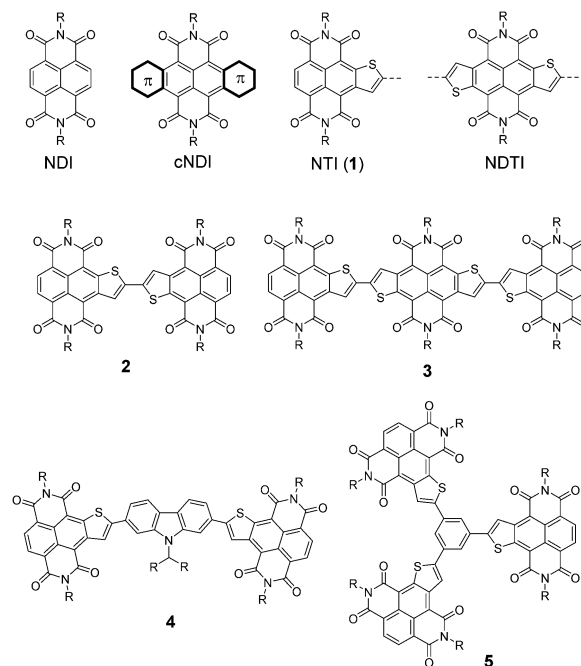


Fig. 1 Chemical structures of naphthalene diimide (NDI), naphtho[2,3-*b*]thiophene diimide (NTI, **1**), naphtho[2,3-*b*:6,7-*b'*]dithiophene diimide (NDTI), and NTI-terminated molecules (**2–5**).

conjugated oligomers and polymers.⁵ We here first report the synthesis and characterization of NTI, and then its utilization to develop a range of NTI-terminated molecular architectures, such as the dimer (**2**), NTI-based triads (**3**, **4**), and a dendritic trimer with a benzene core (**5**), which acted as n-type organic semiconductors (Fig. 1).

For the synthesis of **1**, we first prepared *N,N'*-dioctyl-2-(trimethylsilyl)ethynyl-NDI (**7a**) from the corresponding 2-bromo-NDI (**6a**, see the ESI†).⁶ As depicted in Scheme 1, **7a** was effectively converted into the NTI structure with a trimethylsilyl (TMS) group at the thiophene α -position (**8a**) in 65% isolated yield *via* a sodium sulphide-promoted thiophene annulation reaction.⁷

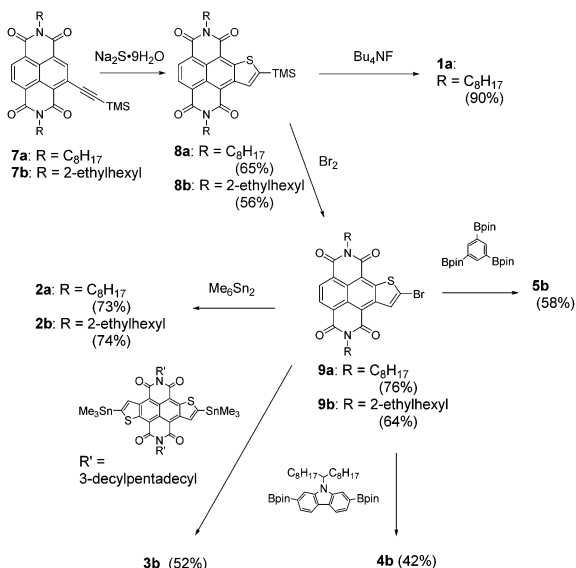
^a Emergent Molecular Function Research Group, RIKEN Center for Emergent Mater Science (CEMS), 2-1, Hirosawa, Wako, Saitama, 351-0198, Japan.

E-mail: masahiro.nakano@riken.jp, takimiya@riken.jp

^b School of Materials Science and Engineering, Nanyang Technological University, 50 Nanyang Avenue, Singapore 639798, Singapore

^c Institute for Sports Research, Nanyang Technological University, 50 Nanyang Avenue, Singapore 639798, Singapore

† Electronic supplementary information (ESI) available. CCDC 1497946. For ESI and crystallographic data in CIF or other electronic format see DOI: 10.1039/c6tc03476d



Scheme 1 Synthesis of NTI (1) and its derivatives (2–5).

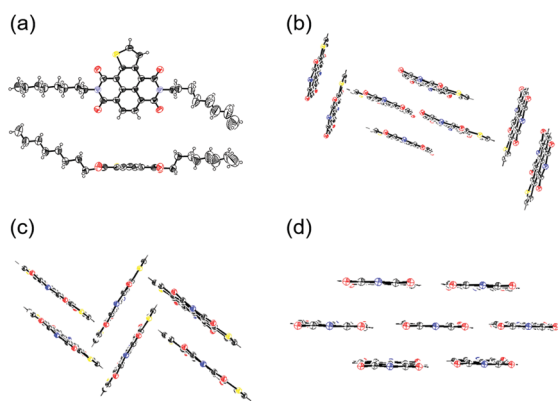


Fig. 2 (a) ORTEP drawing (50% probability) of molecular structure of 1a. Note that the sulphur atom in the thiophene ring is disordered by ca. 30%, and only the major one is depicted. (b) Packing structure of 1a, (c) NDTI (R = C_8H_{17}), and (d) NDI (R = C_6H_{13}). Their alkyl groups are omitted for clarity.

The TMS group was readily removed to give 1a (90% yield), which was fully characterized by spectroscopic analysis (see the ESI†) and single crystal X-ray analysis (Fig. 2a). Although the position of the sulphur atom in the thiophene ring is disordered in the crystal, the almost planar molecular structure is confirmed as its analogous compound, NDTI. Interestingly, the packing motif of NTI shows the characteristics of both NDI and NDTI (Fig. 2b); at the fused-thiophene side, the NTI molecules crystallise in a “face-to-edge” manner, similar to the packing motif that was observed in the crystal structure of NDTI (Fig. 2c).^{5a} On the other hand, at the side without the annulated-thiophene ring, the intermolecular hydrogen bonds between the hydrogen atom of the naphthalene core and the imide carbonyl group is observed, which is reminiscent of the packing structure of NDI (Fig. 2d).⁸

The TMS-substituted NTI (8a) was converted into the corresponding bromide (9a) in a 76% isolated yield by the treatment

with bromine. A reaction of 9a with hexamethylditin in the presence of tetrakis(triphenylphosphine)palladium gave the dimer 2a as a poorly soluble maroon solid. Similar palladium-catalysed coupling reactions of 9a with stannylated or borylated π -units, however, turned out to be useless, because of the extremely poor solubility of the desired products. This is likely due to their planar and rigid structure originating from the effective conjugation through the thiophene α -position. In order to improve the solubility of the resulting products, we introduced 2-ethylhexyl groups on the NTI core. As a result, the corresponding dimer (2b), triads (3b, 4b), and trimer (5b) were readily synthesized and isolated as a pure form in reasonable yields (Scheme 1).

The optoelectronic properties of the NTI and its derivatives were elucidated by absorption/photoluminescence spectroscopy and solution electrochemistry. 1a shows an absorption band (λ_{max} : 482 nm), which is between those of NDI (λ_{max} : 379 nm) and NDTI (λ_{max} : 548 nm) (Fig. 3a). This can be qualitatively understood by the fact that the thiophene-annulation increases the energy level of the highest occupied molecular orbital (HOMO) without significant perturbation to the energy level of the lowest unoccupied molecular orbital (LUMO). This trend was reproduced by the theoretical calculations using DFT methods (Fig. S1, ESI†). Interestingly, 1a shows intensive fluorescence with a high quantum efficiency (ϕ_{PL} : 0.85, Fig. 3c and Table 1), which is markedly or slightly higher than that of the corresponding NDI (ϕ_{PL} : lower than the detectable limit by our hands) or NDTI (ϕ_{PL} : 0.76), respectively. Extension of the conjugation system by the accumulation of the NTI cores brings about bathochromic shifts; the absorption maximum of the dimer (2b) and trimer (3b) shifts to 543 nm and 622 nm, respectively, whereas that of the trimer with the benzene core (5b) is 506 nm (Fig. 3b). This is clearly explained by the nature of connection of the NTI units; for 2b and 3b, the thiophene–thiophene junction(s) allows quite effective conjugation, whereas the benzene linker through its *meta*-positions is less effective for the electronic communication between the NTI units, resulting in a smaller extent of bathochromic shift. On the other hand, the accumulation of three NTI units enhances the extinction coefficient of 5b relative to those of NTI (1a) and dimer (2b) (Table 1). Additionally, the triad with the acceptor–donor–acceptor (A–D–A) structure (4b) also showed bathochromically shifted absorption. Although the quantum yields are not very high, all these NTI derivatives showed orange to red fluorescence, which indicates that NTI is a potential building block for developing red to near-infrared (NIR) fluorescent dyes (Fig. 3d).

As predicated by the theoretical calculations (Fig. S1, ESI†), the LUMO energy levels (E_{LUMO}) are not significantly affected by the thiophene annulation on the NDI core; the electrochemically estimated E_{LUMO} values of NDI (−3.8 eV), NTI (1a, −3.9 eV) and NDTI (−4.0 eV) are only slightly different (Fig. 3e and Table 1). Meanwhile, the E_{LUMO} values of the NTI derivatives can be tuned by the accumulation manner of the NTI units; the direct dimerization of two NTI units efficiently lowers the E_{LUMO} (2b, −4.1 eV), which is again explained by the effective conjugation of two NTIs through the thiophene–thiophene junction. Similarly, the NTI–NDTI–NTI triad (3b) with the thiophene–thiophene



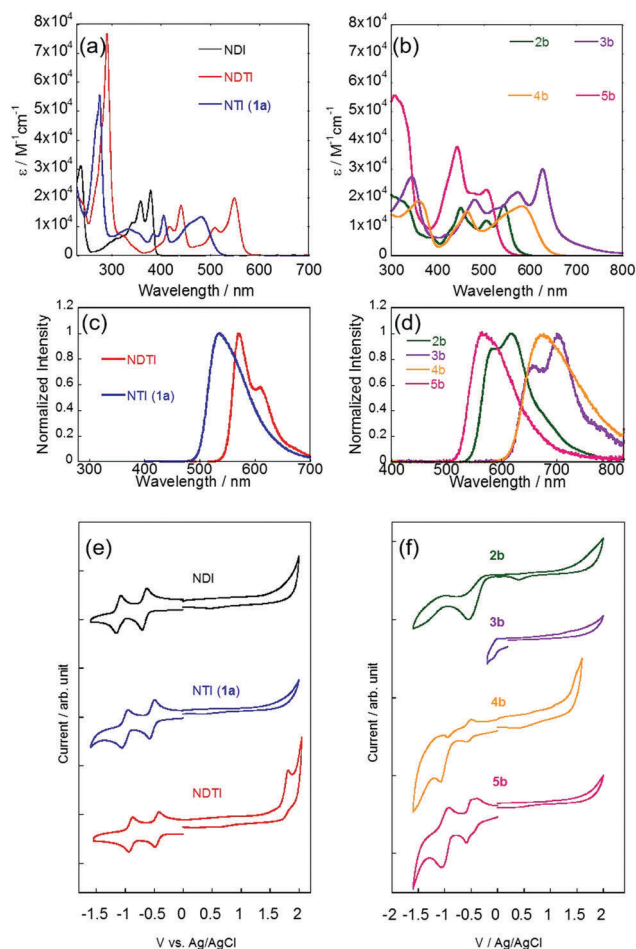


Fig. 3 Absorption spectra (a and b), fluorescence spectra (c and d) and cyclic voltammograms (e and f) of NDI, NTI (1a), NDTI, NTI dimer (2b), triads (3b, 4b), and trimer (5b). Note that the poor solubility of 3b made it difficult to observe the second or higher reduction waves. See the ESI† for further details.

junctions showed a much anodically shifted reduction wave, corresponding to its E_{LUMO} of -4.3 eV. On the other hand, the E_{LUMO} of 5b, which has three identical NTI units, is only slightly lowered (by ca. 0.1 eV), owing to less effective conjugation between NTI units through the benzene *meta*-position (Fig. 3f). The shape of the reduction wave in the voltammograms is also affected by the manner of accumulation of NTI units. 2b showed an

irreversible reduction wave with the onset at -0.26 V (vs. Ag/AgCl), which is ascribed to the formation of radical anion species. However, during the voltammogram measurements, the working electrode was covered with a black solid, indicating that the radical anion species was deposited as a radical anion salt, which caused the disappearance of the corresponding oxidation wave from the radical anion to the neutral state in the cyclic voltammogram. On the other hand, 5b showed quasi-reversible multiple reduction processes, in sharp contrast to the simple two-stage stepwise reduction process of NTI (1a). With the aid of a differential pulse voltammetry (DPV) technique (Fig. S2a, ESI†), we assigned the reduction processes of 5b as follows; the first reduction process is one-electron reduction (half-wave reduction potential, $E_{\text{red}}^{1/2} = -0.40$ V), which is followed by a two-electron reduction process at $E_{\text{red}}^{1/2} = -0.50$ V, resulting in triple NTI-mono-anions, and then the second reduction of each NTI unit occurs simultaneously as a three-electron reduction process at $E_{\text{red}}^{1/2} = -0.90$ V to create the triple NTI-dianions (Fig. S2b, ESI†). It is interesting to note that similar but slightly different stepwise redox behaviors were reported for several NDI trimers.⁹

As clearly demonstrated by the electrochemical evaluations, the NTI derivatives with low-lying E_{LUMO} s seem to be promising as n-type organic semiconductors similar to recently reported NDI-terminated semiconducting materials.¹⁰ To confirm the utility of these NTI derivatives as organic semiconductors, we took 2b, 3b, 4b, and 5b as the model compounds for device applications. We assumed that 2b and 3b with linear molecular structures should be suitable as the active materials in thin-film transistors, as the related naphtho[*b*]thiophene dimer or naphtho[*b*]thiophene-substituted NDTI derivatives behave as decent organic semiconductors for hole or electron transport.^{4d,11} We thus first fabricated 2b- and 3b-based field-effect transistors by vapor-deposition and spin-coating, respectively, on Si/SiO₂ substrates modified with octadecyltrichlorosilane (ODTS) (see the ESI†). As expected, the devices operated under ambient conditions, and the extracted electron mobility was 0.43 and 0.10 cm² V⁻¹ s⁻¹, respectively (Fig. S4, S5, and Table S1, ESI†). Although the electron mobility is moderate, their capability of operation under ambient conditions is a positive sign for further optimization of the molecular structure to develop better n-type organic semiconductors. On the other hand, NTI derivatives with the A-D-A triad (4b) or dendritic trimer with a C_{3h} symmetry (5b) seem to be interesting as an acceptor molecule for

Table 1 Physicochemical properties of NDI, NDTI, NTI, and NTI derivatives

| Comp. | $E_{\text{red}}^{\text{onset a/V}}$ | $E_{\text{LUMO}}^{\text{b/eV}}$ | $E_{\text{oxi}}^{\text{onset a/V}}$ | $E_{\text{HOMO}}^{\text{b/eV}}$ | λ_{max} (log ε)/nm | $\lambda_{\text{edge}}/\text{nm}$ | $E_{\text{g}}^{\text{opt c/eV}}$ | $\lambda_{\text{PL}}^{\text{max}}/\text{nm}$ | $\phi_{\text{PL}}^{\text{d}}$ |
|-------------------|-------------------------------------|---------------------------------|-------------------------------------|---------------------------------|-----------------------------------|-----------------------------------|----------------------------------|--|-------------------------------|
| NTI (1a) | -0.48 | -3.9 | — | — | 482 (4.13), 407 (4.14) | 510 | 2.4 | 537 | 0.85 |
| 2b | -0.26 | -4.1 | — | — | 543 (4.25), 451 (4.22) | 575 | 2.1 | 617 | 0.26 |
| 3b | -0.01 | -4.3 | — | — | 627 (4.48), 573 (4.34) | 680 | 1.8 | 701 | 0.10 |
| 4b | -0.47 | -3.9 | +1.37 | -5.8 | 582 (4.23), 465 (4.19) | 630 | 2.0 | 674 | 0.21 |
| 5b | -0.34 | -4.0 | — | — | 506 (4.36), 442 (4.58) | 540 | 2.3 | 566 | 0.11 |
| NDI ^e | -0.59 | -3.8 | — | — | 379 (4.35), 360 (4.28) | 390 | 3.1 | — | — |
| NDTI ^e | -0.36 | -4.0 | +1.71 | -6.1 | 548 (4.30), 510 (4.29) | 570 | 2.1 | 569 | 0.76 |

^a V vs. Ag/AgCl. Cyclic voltammograms (CVs) were recorded in benzonitrile containing tetrabutylammonium hexafluorophosphate (Bu₄NPF₆, 0.1 M) as supporting electrolyte at a scan rate of 100 mV s⁻¹. ^b Electrochemical E_{LUMO} s/ E_{HOMO} s were estimated from E (eV) = $-4.4 - E_{\text{onset}}$. ^c Estimated from the absorption edge. ^d Absolute quantum yield. ^e Alkyl groups on the imide nitrogen atoms are *n*-octyl group.



solar cells.¹² We thus fabricated solar cells consisting of a bulk heterojunction layer made with a 1:1 equimolar mixture of poly[4,8-bis(5-(2-ethylhexyl)thiophen-2-yl)benzo[1,2-*b*;4,5-*b'*]dithiophene-2,6-diyl-*alt*-(4-(2-ethylhexyl)-3-fluorothieno[3,4-*b*]thiophene)-2-carboxylate-2,6-diyl] (PTB7-Th)¹³ and **4b** or **5b** as the p- and n-type material, respectively. As demonstrated by the absorption spectrum of each component, in particular, **5b** and PTB7-Th show complementary absorption bands effectively covering almost the whole visible range (400–800 nm, see Fig. S8, ESI†). Although the power conversion efficiency was not comparable to the state-of-the-art, both **4b** and **5b** served as small-molecular nonfullerene acceptors in the organic solar cells (Fig. S7 and Table S2, S3, ESI†, PCE for PTB7-Th/**4b**: 1.9%, PTB7-Th/**5b**: 2.5%). Note that these performances are similar to those of the NDI-based small molecule recently developed,¹⁴ which implies that NTI is a promising building block for non-fullerene acceptors.

In summary, we have successfully synthesized naphtho[2,3-*b*]thiophene diimide (NTI). The characteristic feature of NTI is a relatively low-lying E_{LUMO} , bathochromically shifted absorption, and strong fluorescence compared to NDI. Moreover, its selective mono-functionalizability at the thiophene α -position enables us to integrate NTI into a range of electron deficient architectures; from a simple dimer, and a linear trimer through thiophene–thiophene junctions, to an A–D–A triad and dendritic trimer with a central benzene core. They worked as n-type organic semiconducting materials for thin-film transistors or solar cells, which indicates that the NTI unit is a useful building block for various electron-deficient molecular architectures. Further design and synthesis of NTI-based n-type organic semiconductors and their utilization in optoelectronic devices are now underway in our group.

We acknowledge the financial support from JSPS KAKENHI Grant Numbers 15H02196 and 16K05900, the Strategic Promotion of Innovative Research and Development from JST, and Iketani Science and Technology Foundation. HRMSs were carried out at the Molecular Structure Characterization Unit, RIKEN Center for Sustainable Resource Science (CSRS). DFT calculations using Gaussian 09 were performed by using the RIKEN Integrated Cluster of Clusters (RICC).

Notes and references

- (a) F. Würthner, S. Ahmed, C. Thalacker and T. Debaerdemaeker, *Chem. – Eur. J.*, 2002, **8**, 4742; (b) N. Sakai, J. Mareda, E. Vauthey and S. Matile, *Chem. Commun.*, 2010, **46**, 4225; (c) S.-L. Suraru and F. Würthner, *Angew. Chem., Int. Ed.*, 2014, **53**, 7428.
- (a) S. Katsuta, K. Tanaka, Y. Maruya, S. Mori, S. Masuo, T. Okujima, H. Uno, K. Nakayama and H. Yamada, *Chem. Commun.*, 2011, **47**, 1011; (b) F. Doria, M. Antonio, M. Benotti, D. Verga and M. Freccero, *J. Org. Chem.*, 2009, **74**, 8616; (c) H. Langhals and S. Kinzel, *J. Org. Chem.*, 2010, **75**, 7781; (d) X. Chen, Y. Guo, L. Tan, G. Yang, Y. Li, G. Zhang, Z. Liu, W. Xu and D. Zhang, *J. Mater. Chem. C*, 2013, **1**, 1087; (e) Y. Hu, X. Gao, C. Di, X. Yang, F. Zhang, Y. Liu, H. Li and D. Zhu, *Chem. Mater.*, 2011, **23**, 1204; (f) J. Gao, Y. Li and Z. Wang, *Org. Lett.*, 2013, **15**, 1366; (g) S.-L. Suraru, C. Burschka and F. Würthner, *J. Org. Chem.*, 2014, **79**, 128; (h) C. Li, C. Xiao, Y. Li and Z. Wang, *Org. Lett.*, 2013, **15**, 682; (i) Q. Ye, J. Chang, K.-W. Huang, X. Shi, J. Wu and C. Chi, *Org. Lett.*, 2013, **15**, 1194; (j) B. Leng, D. Lu, X. Jia, X. Yang and X. Gao, *Org. Chem. Front.*, 2015, **2**, 372; (k) D. Lu, X. Yang, B. Leng, X. Yang, C. Ge, X. Jia and X. Gao, *Chin. Chem. Lett.*, 2016, **27**, 1022; (l) X. Gao and Y. Hu, *J. Mater. Chem. C*, 2014, **2**, 3099.
- A. C. Thompson, H. M. Grimm, A. G. Bè, K. J. McKnight and J. J. Reczek, *Synth. Commun.*, 2015, **45**, 1127. Note that the effective synthesis of mono-brominated naphthalene-1,4,5,8-tetracarboxylic anhydride, which is a suitable starting material for mono-aromatic fused cNDIs, was already reported. However, we were not able to reproduce the results.
- (a) C. B. Nielsen, S. Holliday, H.-Y. Chen, S. J. Cryer and I. McCulloch, *Acc. Chem. Res.*, 2015, **48**, 2803; (b) Q. Yan, Y. Zhou, Y.-Q. Zheng, J. Pei and D. Zhao, *Chem. Sci.*, 2013, **4**, 4389; (c) D. Zhao, Q. Wu, Z. Cai, T. Zheng, W. Chen, J. Lu and L. Yu, *Chem. Mater.*, 2016, **28**, 1139; (d) J. Yi, Y. Wang, Q. Luo, Y. Lin, H. Tan, H. Wang and C.-Q. Ma, *Chem. Commun.*, 2016, **52**, 1649; (e) Q. Wu, D. Zhao, A. M. Schneider, W. Chen and L. Yu, *J. Am. Chem. Soc.*, 2016, **138**, 7248.
- (a) Y. Fukutomi, M. Nakano, J.-Y. Hu, I. Osaka and K. Takimiya, *J. Am. Chem. Soc.*, 2013, **135**, 11445; (b) E. Zhou, M. Nakano, S. Izawa, J. Cong, I. Osaka, K. Takimiya and K. Tajima, *ACS Macro Lett.*, 2014, **3**, 872; (c) M. Nakano, I. Osaka and K. Takimiya, *Macromolecules*, 2015, **48**, 576; (d) M. Nakano, I. Osaka, D. Hashizume and K. Takimiya, *Chem. Mater.*, 2015, **27**, 6418; (e) J.-Y. Hu, M. Nakano, I. Osaka and K. Takimiya, *J. Mater. Chem. C*, 2015, **3**, 4244; (f) K. Nakano, M. Nakano, B. Xiao, E. Zhou, K. Suzuki, I. Osaka, K. Takimiya and K. Tajima, *Macromolecules*, 2016, **49**, 1752; (g) M. Nakano, M. Sawamoto, M. Yuuki and K. Takimiya, *Org. Lett.*, 2016, **18**, 3370; (h) M. Nakano, D. Hashizume and K. Takimiya, *Molecules*, 2016, **21**, 981.
- (a) B. A. Jones, A. Facchetti, T. J. Marks and M. R. Wasielewski, *Chem. Mater.*, 2007, **19**, 2703; (b) S. F. Volker, A. Schmiedel, M. Holzapfel, C. Bohm and C. Lambert, *Phys. Chem. Chem. Phys.*, 2013, **15**, 19831.
- (a) D. S. Baranov, B. Gold, S. F. Vasilevsky and I. V. Alabugin, *J. Org. Chem.*, 2013, **78**, 2074; (b) L. G. Fedenok, K. Y. Fedotov, E. A. Pritchina and N. E. Polyakov, *Tetrahedron Lett.*, 2016, **57**, 1273.
- D. Shukla, S. F. Nelson, D. C. Freeman, M. Rajeswaran, W. G. Ahearn, D. M. Meyer and J. T. Carey, *Chem. Mater.*, 2008, **20**, 7486.
- (a) L. E. Polander, A. S. Romanov, S. Barlow, D. K. Hwang, B. Kippelen, T. V. Timofeeva and S. R. Marder, *Org. Lett.*, 2012, **14**, 918; (b) S. T. Schneebeli, M. Frasconi, Z. Liu, Y. Wu, D. M. Gardner, N. L. Strutt, C. Cheng, R. Carmieli, M. R. Wasielewski and J. F. Stoddart, *Angew. Chem., Int. Ed.*, 2013, **52**, 13100.
- (a) Y. A. Getmanenko, L. E. Polander, D. K. Hwang, S. P. Tiwari, E. Galàn, B. M. Seifried, B. Sandhu, S. Barlow,



- T. Timodeeva, B. Kippelen and S. R. Marder, *J. Org. Semicond.*, 2014, **1**, 7; (b) Y. A. Getmanenko, S. Singh, B. Sandhu, C.-Y. Wang, T. Timodeeva, B. Kippelen and S. R. Marder, *J. Mater. Chem. C*, 2014, **2**, 124; (c) L. E. Polander, S. P. Tiwari, L. Pandey, B. M. Seigried, Q. Zhang, S. Barlow, C. Risko, J.-L. Brédas, B. Kippelen and S. R. Marder, *Chem. Mater.*, 2011, **23**, 3408; (d) Z. Wang, X. Li, Y. Zou, J. Tan, X. Fu, J. Liu, C. Xiao, H. Dong, W. Jiang, F. Liu, Y. Zhen, Z. Wang, T. P. Russell and W. Hu, *J. Mater. Chem. C*, 2016, **4**, 7230.
- 11 M. Mamada, J.-i. Nishida, D. Kumaki, S. Tokito and Y. Yamashita, *J. Mater. Chem.*, 2008, **18**, 3442.
- 12 T. V. Pho, F. M. Toma, B. J. T. de Villers, S. Wang, N. D. Treat, N. D. Eisenmenger, G. M. Su, R. C. Coffing, J. D. Douglas, J. M. J. Fréchet, G. C. Bazan, F. Wudl and M. L. Chabinyc, *Adv. Energy Mater.*, 2014, **4**, 1301007.
- 13 (a) S.-H. Liao, H.-J. Jhuo, Y.-S. Cheng and S.-A. Chen, *Adv. Mater.*, 2015, **25**, 4766; (b) S. Zhang, L. Ye, W. Zhao, D. Liu, H. Yao and J. Hou, *Macromolecules*, 2014, **47**, 4653; (c) Z. He, B. Xiao, F. Liu, H. Wu, Y. Yang, S. Xiao, C. Wang, T. P. Russell and Y. Cao, *Nat. Photonics*, 2015, **9**, 174.
- 14 Y. Liu, L. Zhang, H. Lee, H.-W. Wang, A. Santala, F. Liu, Y. Diao, A. L. Briseno and T. P. Russell, *Adv. Energy Mater.*, 2015, **5**, 1500195.

